ACKNOWLEDGMENT

Field tests in the United States to date have been made possible by the interest of J.W. Deskins, Director, Street and Bridge Department and by E.D. Longley, Director of Street Maintenance in Los Angeles. Their interest and cooperation is gratefully acknowledged. The assistance of A.B. De Simon, Chief of Calgary's Plants Operation, and Paul Nemorin are appreciated. Milton F. Masters and Leo Davis of Industrial Asphalt Inc. have provided valuable help in coring and testing the initial Los Angeles test pavements.

Texas stabilometer tests were performed on Houston plant mixes by Southwestern Laboratories, Inc. LaBelle Consultants measured stability of the recent Los Angeles pavements by using standard California procedures. The Chicago Testing Laboratory ran Marshall stability tests on Calgary plant mixes and performed extraction-recovery tests on all pavement cores reported herein.

REFERENCES

1. H.W. Skidmore and J. Donohue. Special Sheet Asphalt Floors in Industrial Plant at Kohler, Wisconsin. Engineering and Contracting, March 1928.
2. B.F. Kallas and H.C. Krieger. Effects of Consistency of Asphalt Cements and Types of Mineral Fillers on the Compaction of Asphalt Concrete. Proc., Association of Asphalt Paving Technologists, Vol. 29, 1960, pp. 162-172.
3. B.F. Kallas and V.P. Puzinauskas. A Study of Mineral Fillers in Asphalt Paving Mixtures. Proc., Association of Asphalt Paving Technologists, Vol. 30, 1961, pp. 493-538.
4. D. Tamburo and J.H. Kietzman. The Effect of Asbestos Fibers on Structural Properties of Asphalt Pavement. Proc., Association of Asphalt Paving Technologists, Vol. 31, 1962.
5. F.L. Raschig and P.C. Doyal. An Extension of Asphalt Research as Reported in the 1937 Proceedings. Proc., Association of Asphalt Paving Technologists, Vol. 9, 1937.
6. P. Hubbard and E.H. Gollomb. The Hardening of Asphalt with Relation to Development of Cracks in Asphalt Pavements. Proc., Association of Asphalt Paving Technologists, Vol. 9, 1937.
7. V.A. Endersby, F.H. Stross, and T.K. Miles. The Durability of Road Asphalts. Proc., Association of Asphalt Paving Technologists, Vol. 14, 1942.
8. N.A. Huculak. Experience with Asbestos in Asphalt Pavement: 6 Year Performance. Canadian Department of Public Works, 1973.
9. E. Tons and G.G. Henault. Evaluation of Micro Aggregates by Smith Triaxial Test. Bull. 329. HRB, National Research Council, Washington, D.C., 1962, pp. 48-63.

Publication of this paper sponsored by Committee on Characteristics of Nonbituminous Components of Bituminous Paving Mixtures.

Combo Viscoelastic-Plastic Modeling and Rutting of Asphaltic Mixtures

A. ABDULSHAFI and KAMRAN MAJIDZADEH

ABSTRACT

Constitutive equations used in solving the boundary value problem of flexible pavements employ linear elastic or viscoelastic theory. Accordingly, permanent deformations are calculated based on elastic or viscoelastic deformation laws. Advances in the field of constitutive modeling of materials indicated the need to develop a constitutive relationship that better replicates asphaltic mixture responses under various loading and environmental conditions. In this paper a one-dimensional combo viscoelastic-plastic constitutive model composed of Burger-type mechanical elements connected in series with a friction slider is used. The friction slider is the mechanical representation of plasticity with a Drucker-Prager yield criterion. This model is solved under creep phase loading conditions, and the solution is used to develop a rutting model that incorporates a densification phase represented by a relaxing spring. Within the verification of the constitutive model a true yield line has been identified and used instead of the Mohr-Coloumb failure line. The two developed models are supplemented by appropriate experimentation phases to identify and numerically evaluate the relevant parameters. Experimentation is based on actual existing routine methods, with proper adjustments, modifications, or extensions to comply with proper evaluation of the model parameters, and kept as simple as possible to encourage wider user acceptance. An example using actual data is worked out and compared with results obtained from the VESYS III structural subsystem program.

Flexible pavements have traditionally been designed as multilayer elastic systems, in which each layer is assumed to be isotropic and homogeneous. Alternatively, the design could be based on an equivalent full-depth asphaltic concrete layer constructed by using layer equivalency concepts. Design techniques are based on analytical study of quasi-static algorithms with loading conditions of a slow-moving vehicle.

Design approaches based on performance were introduced in the early 1970s and are based on designing a flexible pavement to guard against functional or structural failures. Functional failures are more subjective in nature because they are associated with road user riding quality. Structural failures are dominantly caused by rutting (or permanent deformation) or fatigue cracking (1,2). These observed distress failures introduced a set of empirical laboratory-evaluated equations that were then raised to the phenomenological level by correlating their coefficients with the material constitutive system constants and loading conditions. In addition, mechanistic models have been proposed and applied to the design, thereby contributing to a better understanding of the damaging mechanisms involved, especially for fatigue cracking (3-5).

Advances in the fields of material characterization and fracture mechanics necessitated more research investigations in the area of flexible pavement structural failures, particularly the development of constitutive relationships that better replicate material responses such as viscoelasticity and viscoplasticity (i.e., viscous-elasic-plastic elements combined in any configuration) with and without yield surfaces, which describe cracking mechanisms such as elastoplastic fracture mechanics. Viscoelastic characterization of asphaltic materials has been investigated (6-9), and computer programs that input the creep compliance or relaxation modulus have been implemented (10,11). Viscoplasticity with yield surface as a constitutive relationship has been developed in the field of solid mechanics (12-15) and has recently been applied to soils (16).

Rutting and fatigue are major field problems. Rutting has been extensively studied at the empirical and phenomenological levels (2,11,17-19), with no attempt to characterize the asphalt mix as other than linear elastic or viscoelastic. Accumulations of permanent deformation were calculated by using elastic and viscous deformation laws. Thus it is not surprising that unsatisfactory correlations with actual field performance still exist; however, these correlations could be improved if concepts such as those previously cited were used.

The objective of this paper is to attempt to bridge part of the existing gap in correlation between laboratory and field performance by outlining and discussing the development of a viscoelastic-plastic constitutive relationship to characterize asphalt mixtures and to predict rutting. The fatigue problem will be addressed separately in a future paper.

VISCOELASTIC-PLASTIC MODELING OF ASPHALTIC MIXTURES

The total strain of asphaltic mixtures under a single impulse load can be decomposed into a recoverable part (elastic and viscoelastic) and a nonrecoverable part (viscous and plastic). By using vectorial notations, this is written as

$$\underset{\sim}{\epsilon}(t) = (\underset{\sim}{\epsilon}_E + \underset{\sim}{\epsilon}_{ve})_{recoverable} + (\underset{\sim}{\epsilon}_v + \underset{\sim}{\epsilon}_{PL})_{nonrecoverable} \quad (1)$$

where

$\underset{\sim}{\epsilon}(t)$ = total strain response vector;

$\underset{\sim}{\epsilon}_E$ = elastic strain vector (time independent), recoverable;

$\underset{\sim}{\epsilon}_{ve}(t)$ = viscoelastic strain vector (time dependent), recoverable;

$\underset{\sim}{\epsilon}_v(t)$ = viscous strain vector (time dependent), nonrecoverable; and

$\underset{\sim}{\epsilon}_{PL}$ = plastic strain vector (time independent), nonrecoverable.

Because plastic strains are preceded by elastic or viscoelastic response, it is instructive to rearrange the terms in Equation 1 as follows:

$$\underset{\sim}{\epsilon}(t) = (\underset{\sim}{\epsilon}_v + \underset{\sim}{\epsilon}_{ve}) + (\underset{\sim}{\epsilon}_E + \underset{\sim}{\epsilon}_{PL}) = \underset{\sim}{\epsilon}_{VE} + \underset{\sim}{\epsilon}_{EP} \quad (2)$$

where, in this equation, $\underset{\sim}{\epsilon}_{VE}$ represents both the recoverable and nonrecoverable parts of the viscoelastic strain response and $\underset{\sim}{\epsilon}_{EP}$ represents an elastic recoverable strain response associated with nonrecoverable plastic strain response. In fact, this arrangement lumps the time-dependent response in a viscoelastic element and the time-independent response in an elastoplastic element. In the following sections, a viscoelastic-plastic constitutive model will be developed based on this strain decomposition.

Elastic-Plastic Strain Response

It is generally assumed that plastic deformation (yielding) does not commence before the stress path reaches a surface in the stress space called the yield surface. The total elastic-plastic strain response for a stress state on the yield surface is made up from the contributions of an elastic response within the yield surface added to the plastic response. Mathematically stated,

$$\underset{\sim}{\epsilon}_{EP} = \underset{\sim}{\epsilon}_E + \underset{\sim}{\epsilon}_{PL} \quad (3)$$

Further, at any stress level, the total stress is related to the elastic strain through Hook's law as follows:

$$\underset{\sim}{\sigma} = \underset{\sim}{D}_E \cdot \underset{\sim}{\epsilon}_E \quad (4)$$

where $\underset{\sim}{\sigma}$ is the total stress vector and $\underset{\sim}{D}_E$ is the elastic constitutive matrix. By substituting Equation 4 into Equation 3, it can be rearranged to obtain

$$\underset{\sim}{\sigma} = \underset{\sim}{D}_E(\underset{\sim}{\epsilon}_{EP} - \underset{\sim}{\epsilon}_{PL}) \quad (5)$$

The next step is to eliminate the plastic strain response in a similar manner; however, this requires understanding the assumptions of the theory of plasticity. The four cornerstones of the classical theory of plasticity are based on the existence of a yield condition, a surface hardening condition, a flow rule, and a hardening rule, as discussed in the following list (1 through 4).

1. The yield condition is a scalar function to determine the onset of plastic deformation. It can be written in the form (20):

$$F(\underset{\sim}{\sigma}, \underset{\sim}{K}, \underset{\sim}{\epsilon}_{PL}, k) = f(\underset{\sim}{\sigma}, \underset{\sim}{K}, \underset{\sim}{\epsilon}_{PL}) - \langle k \rangle = \begin{cases} <0 \text{ no yielding} \\ 0 \text{ onset of yielding} \\ >0 \text{ unattainable} \end{cases} \quad (6)$$

where

$F(\underset{\sim}{\sigma}, \underset{\sim}{K}, \underset{\sim}{\epsilon}_{PL}, k)$ = yield condition,

$\underset{\sim}{\sigma}$ = any stress state on the yield surface,

$\underset{\sim}{K}$ = prestress state that generated the present yield surface,
$\underset{\sim}{\varepsilon}_{PL}$ = plastic strain,
$\underset{\sim}{k}$ = yield parameter,
$f(\underset{\sim}{\sigma}, \underset{\sim}{K}, \underset{\sim}{\varepsilon}_{PL})$ = loading function, and
<k> = yield parameter that can be a function of the plastic strain.

The loading function is usually chosen referenced to the invariant stress space. In multidimensional stress space, the vector argument of the loading function allows much freedom in choosing its form to suit the required material characteristics. For example, if plastic flow is not affected by hydrostatic stress, as in the case for most metals, then the loading function could be expressed in terms of the second invariant deviatoric stress, J_2. If, on the other hand, plastic flow is affected by both shear stress and hydrostatic stress, as is usually the case in soils and asphalt mixes, then the loading function would more appropriately be expressed in terms of both the first and second invariants of stress. Further, the loading function serves as a test for whether or not plastic deformation occurs. For F = 0, the current stress state is on the yield surface, and for an increment of stress $d\underset{\sim}{\sigma}$ (which could be in a direction different from that of the outward normal to the yield surface, $\hat{\underset{\sim}{n}}$), the equation is

$$(\partial \underset{\sim}{f}/\partial \underset{\sim}{\sigma}) \cdot d\underset{\sim}{\sigma} = \begin{cases} >0 \text{ plastic loading} \\ 0 \text{ neutral loading} \\ <0 \text{ elastic (or viscoelastic) unloading} \end{cases} \tag{7}$$

where $\partial \underset{\sim}{f}/\partial \underset{\sim}{\sigma}$ is the gradient of the loading function; its direction is in the direction of the outward normal to the yield surface, $\hat{\underset{\sim}{n}}$.

2. The surface hardening condition is the law that describes the movement of the yield surface during plastic deformation in the stress space. The yield surface translating in space as a rigid body is kinematic hardening; if it dilates or contracts without either change in shape or translates in space, it is isotropic hardening. Various movements of the yield surface can also be described, such as anisotropic hardening (same as isotropic but with change in shape) or universal (mixed) mode hardening where both isotropic and kinematic hardening are in effect.

3. The flow rule is the relationship between the stress and strain during plastic yielding. The direction of the plastic strain can be normal to the yield surface (associated flow rule) or can be inclined to this surface (nonassociated flow rule). Because plastic strain is a vector in multidimensional space, then its inclination is hypothesized to be due to the fact that not all the loading function is effective in pulling the yield surface, but only a part of it. The acting stress is also a vector in multidimensional space that can be decomposed into effective and noneffective stress vectors. The effective stress vector can evidently have a unit normal in a direction different from that of the whole stress vector.

4. The hardening rule is the mathematical expression that provides the value of the hardening function or coefficient as a measure of thermodynamic state variable, namely, work hardening and strain hardening. The choice between the two is a matter of experimental or calculable convenience.

Because the onset of plastic deformation only needs an increment of stress on the yield surface, it is more sensible to deal with the incremental theory of plasticity. In fact, all of the preceding equations could be obtained in compliance with this theory by replacing $\underset{\sim}{\sigma}$, $\underset{\sim}{\varepsilon}$, t, and so forth by their corresponding increments $d\underset{\sim}{\sigma}$, $d\underset{\sim}{\varepsilon}$, dt, and so forth. The plastic strain increment could be written as

$$d\underset{\sim}{\varepsilon}_{PL} = \lambda \hat{\underset{\sim}{m}} \tag{8}$$

where λ is the magnitude of plastic strain increment, and $\hat{\underset{\sim}{m}}$ is the unit vector in the direction of the plastic strain increment. Based on Prager's assumption (21), the effective stress vector $(\hat{\underset{\sim}{n}} \cdot d\underset{\sim}{\sigma})$ is related to the magnitude of plastic strain increment by the following equation:

$$\lambda = (1/H)(\hat{\underset{\sim}{n}}^T \cdot d\underset{\sim}{\sigma}) \tag{9}$$

where $\hat{\underset{\sim}{n}}^T$ is the transpose of the yield surface outward normal and H is the hardening parameter that could be found experimentally, as will be shown later. Substituting Equation 9 into Equation 8 yields

$$d\underset{\sim}{\varepsilon}_{PL} = (1/H)(\hat{\underset{\sim}{n}}^T \cdot d\underset{\sim}{\sigma})\hat{\underset{\sim}{m}} \tag{10}$$

By some mathematical manipulations (22-24), the following can be obtained:

$$d\underset{\sim}{\sigma} = (\underset{\sim}{D}_E - \underset{\sim}{D}_{PL})d\underset{\sim}{\varepsilon} \tag{11}$$

where

$$\underset{\sim}{D}_{PL} = \underset{\sim}{D}_E \hat{\underset{\sim}{m}} \hat{\underset{\sim}{n}} \underset{\sim}{D}_E/(H + \hat{\underset{\sim}{n}}^T \underset{\sim}{D}_E \hat{\underset{\sim}{m}})$$

Equation 11 is the elastic-plastic constitutive equation in multidimensional stress space.

Model Development for Asphaltic Mixtures

To devise a simple test to obtain the required parameters that characterize the elastic-plastic response behavior of asphalt mixes, Equation 11 must be reduced to a one-dimensional equivalent. Figure 1

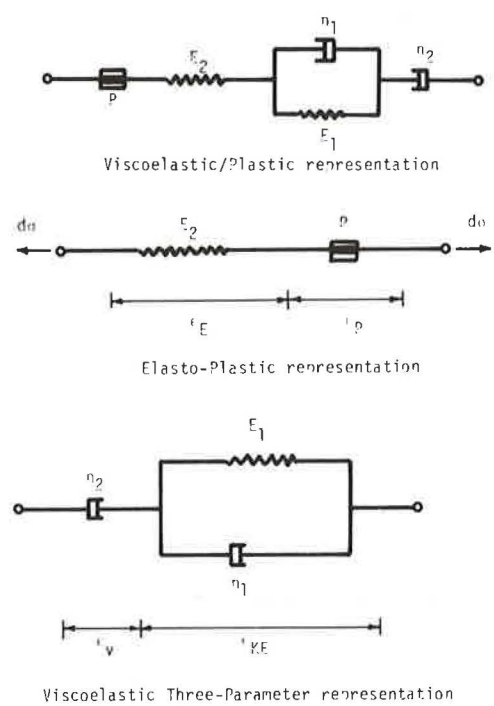

FIGURE 1 One-dimensional mechanical models.

shows a one-dimensional mechanical model representation. The following assumptions are made:

1. Yield condition: $F = F(\underset{\sim}{\sigma}, K) = F(\underset{\sim}{\sigma}) - K$
   (a) Yield parameter: isotropic hardening, $K = K_o + \Delta K$
   (b) Loading function:
      (i) Von Mises--$f(\underset{\sim}{\sigma}) = \sqrt{J_2'}$
      (ii) Drucker-Prager--$f(\underset{\sim}{\sigma}) = \alpha I_1 + \sqrt{J_2'}$
2. Associated flow rule: $\underset{\sim}{\hat{n}} = \underset{\sim}{\hat{m}}$
3. Hardening parameter is a function of the plastic work, $H = H(W_p)$,

where

K = yield parameter (measure the current cone or cylinder radius);
K_o = cone or cylinder radius at initial onset of plastic deformation;
ΔK = increment of increase in cone or cylinder radius due to plastic strain increment;
I_1 = octahedral normal stress = 1st stress invariant = $(1/3)(\sigma_1 + \sigma_2 + \sigma_3)$;
J_2' = 2nd reduced stress invariant = $(1/6)[(\sigma_1 - \sigma_2)^2 + (\sigma_2 - \sigma_3)^2 + (\sigma_3 - \sigma_1)^2]$;
$\sigma_1, \sigma_2, \sigma_3$ = principal stresses; and
α = scalar multiplier that measures the rate of increase of the cone radius along the hydrostatic stress line (the cone centerline).

Note that if $\alpha = 0$, the Drucker-Prager yield condition reduces to that of Von Mises. In conclusion, a Drucker-Prager yield condition is the general case, where α, K, and $H(W_p)$ must be found experimentally to uniquely define an asphalt mix constitutive equation. Cylinderical triaxial tests could be used for that purpose. The stress path of this test fixes a point on the yield surface where Von Mises, Tresca, Drucker-Prager, and Mohr-Coloumb yield surfaces intersect. Thus the use of the Mohr-Coloumb yield criterion to obtain parameters for any of the previous yield conditions is justified. Figure 2 shows a Mohr-Coloumb failure line that can be expressed mathematically as

$$\tau = C + \sigma \tan \phi \tag{12}$$

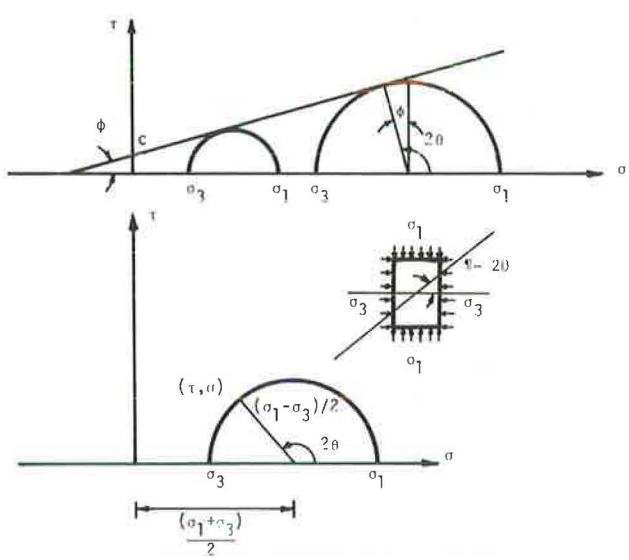

FIGURE 2 Mohr-Coloumb stress state graphical representation.

where

τ = shear stress at failure,
C = cohesion intercept,
σ = normal stress at failure, and
ϕ = angle of internal friction.

Because it is known that

$$\sigma = [(\sigma_1 + \sigma_3)/2] + [(\sigma_1 - \sigma_3)/2] \cos 2\theta \; ; \tau[(\sigma_1 - \sigma_3)/2] \sin 2\theta \tag{13}$$

and by substituting Equation 13 into Equation 12 and doing some rearranging,

$$\sigma_1 - [(1 - \cos 2\theta)/(1 + \cos 2\theta)]\sigma_3 - [(2C \sin 2\theta)/(1 + \cos 2\theta)] = 0 \tag{14}$$

For stress states typical of that found in triaxial tests, $\sigma_2 = \sigma_3$,

$$I_1 = (\sigma_1 + 2\sigma_3)/3 \text{ and } \sqrt{J_2'} = (\sigma_1 - \sigma_3)/3 \tag{15}$$

Substituting Equation 15 into assumption b-ii of the yield condition gives

$$F(\underset{\sim}{\sigma}, K) = (\alpha/3)(\sigma_1 + 2\sigma_3) + (|\sigma_1 - \sigma_3|/\sqrt{3}) - K = 0 \tag{16}$$

The triaxial test previously cited is not currently considered in routine asphalt testing. Thus it is desirable to find the two model parameters (α and K) from other independent tests that are routinely performed, such as direct compression and indirect tension tests. If it is assumed that asphalt mixes are a unimodular material, and by setting $\sigma_3 = 0$ and using some mathematical manipulations (22), then Equation 16 will be reduced to

$$\pm \sigma_1 = 3K_o/[\alpha + \sqrt{3}\, \mathrm{sgn}(\sigma_1)] \tag{17}$$

where $-\sigma_1$ and $+\sigma_1$ are the compressive and tensile ultimate stresses, respectively, and $\mathrm{sgn}(\sigma_1)$ denotes the sign of the major principal stress (uniaxial stress in this case). A major criticism of this scheme is using the Mohr-Coloumb failure line as a yielding line. Fortunately, actual yield points in tension and compression of asphalt mixes can be found by using creep test data. The third quantity to be determined is the hardening parameter, H. For a one-dimensional model, $d\underset{\sim}{\sigma} = d\sigma_1$; $d\underset{\sim}{\varepsilon}_{PL} = d\varepsilon_{PL}$; $\underset{\sim}{\hat{n}} = \underset{\sim}{\hat{m}} = n_1$. Hence by substituting these in Equation 10,

$$H = n_1^2 (d\sigma_1/d\varepsilon_{PL}) \tag{18}$$

where $d\sigma_1/d\varepsilon_{PL}$ is the instantaneous slope of the stress-plastic strain curve, and

$$n_1 = 2[\alpha + \sqrt{3}\, \mathrm{sgn}(\sigma_1)]/\sqrt{6(2\alpha^2 + 3)} \tag{19}$$

The procedure for determining the plasticity parameters α, K, and $H(W_p)$ is as follows:

1. The stress-plastic strain curve is established from appropriate tests by deducting all other strains from the total strains.
2. The slope of the curve is found at selected appropriate points, and these values are multiplied by n_1^2 to get H.
3. Values of the plastic work done ($W_p = \int_0^{\varepsilon} \sigma_1 d\varepsilon$ = area under the $\sigma - \varepsilon_{PL}$ curve) is found, and the curve-fitting H versus W_p is established.
4. This will give $H(W_p)$, which is the required hardening parameter.
5. The values of the α and K parameters could be obtained from creep test data (22) as well as indirect tension and uniaxial compressive strength tests.

Substitute Equation 18 into the incremental equivalents of Equations 3 and 4 to get

$$d\epsilon_{EP} = C_{EP} \cdot d\sigma_1 \tag{20}$$

where

C_{EP} = elastic-plastic compliance = $(1/E_2) + \langle n_1^2/H(W_p)\rangle$

and

$$\langle n_1^2/H(W_p)\rangle = \begin{cases} 0 \text{ if } \sigma < \sigma_{yield} \\ n_1^2/H(W_p) \text{ if } \sigma \geq \sigma_{yield} \end{cases}$$

Equation 20 is the governing equation for the response of the elastic-plastic element.

Viscoelastic Strain Responses

Figure 1 includes the one-dimensional viscoelastic element to be solved. The governing differential operator equation is easily found to be (22)

$$[E_1 \eta_2 (d/dt) + \eta_1 \eta_2 (d^2/dt^2)]\ \epsilon_{VE} = [E_1 + (\eta_1 + \eta_2)(d/dt)]\ \sigma_1 \tag{21}$$

where d/dt is the time derivative. Because creep tests will be used for model verification, then by imposing incremental creep phase loading conditions, $d\sigma_1 = d\sigma$ = const., Equation 21 will yield the following solution:

$$d\epsilon_{VE}(t) = C_{VE}\, d\sigma_1 \tag{22}$$

where

C_{VE} = viscoelastic compliance = $(t/\eta_2) + (1/E_1)\{1 - EXP[-(E_1/\eta_1)t]\}$,
t = time scale,
E_1 = uniaxial elastic spring coefficient, and
η_1, η_2 = viscous coefficients of the corresponding dashpots.

Equation 22 is in the form of the required viscoelastic strain response.

Viscoelastic-Plastic Strain Response

Substitute Equations 20 and 22 into Equation 2 to obtain

$$d\epsilon_1(t) = C_{VEP}\, d\sigma_1 \tag{23}$$

where C_{VEP} is the viscoelastic-plastic compliance, that is,

$$C_{VEP} = \left(\left\{(1/E_2) + (t/\eta_2) + (1/E_1)[1 - EXP(-E_1/\eta_1)t]\right\} + \langle [n_1^2/H(W_p)]\rangle\right)$$

Equation 23 represents the mathematical relationship of the viscoelastic-plastic mechanical model for asphalt mixes, where the parameters E_1, E_2, η_1, η_2, α, K, n_1, and $H(W_p)$ could be found experimentally.

Rutting or Permanent Deformation Model

Rutting is defined as the accumulation of permanent deformation in the wheel path and is caused by one or more of the following mechanisms: densification, viscous flow, and plastic deformation. If no interaction is assumed among these mechanisms, then the one-dimensional mathematical relationship that describes the permanent deformation will be

$$\epsilon_p = \epsilon_{p_o} + \epsilon_v(t) + \epsilon_{PL} \tag{24}$$

where

ϵ_p = permanent total deformation;
ϵ_{p_o} = permanent deformation due to densification; it could be represented by an in-series mechanical relaxing spring with constant E_{p_o};
$\epsilon_v(t)$ = time-dependent viscous permanent deformation; and
ϵ_{PL} = time-independent plastic permanent deformation.

By using the relevant elements of the viscoelastic-plastic model, Equation 24 could be written as

$$\epsilon_p = C_p \cdot \sigma_1 \tag{25}$$

where

$C_p = \{(1/E_{p_o}) + (t/\eta_2) + \langle [n_1^2/H(W_p)]\rangle\}$,
$\sigma_1 = \begin{cases} \sigma_c \text{ in uniaxial compression} \\ \sigma_t \text{ in uniaxial tension,} \end{cases}$
E_{p_o} = densification spring modulus, and
η_2 = coefficient of viscosity of the in-series dashpot.

Equation 25 represents permanent deformation caused by a constant stress-loading condition acting for an arbitrary time t. An immediate permanent deformation due to densification will occur and may or may not be accompanied by plastic deformation, depending on the magnitude and sign of the stress. Contrary to that, the permanent viscous deformation is effective only after a time step is defined. On the other hand, experimental testing for rutting establishes the relationship between the permanent deformation per cycle (ϵ_p) and the number of cycles (N) at the measured values of ϵ_p by procedures found elsewhere in the literature (11,19,25). The general form of this relationship is

$$\epsilon_{p_{acc}} = \epsilon'_{p_{acc}}/N = K_1 N^{-m} \tag{26}$$

where

$\epsilon_{p_{acc}}$ = average accumulated permanent deformation per cycle,
$\epsilon_{p_{acc}}'$ = accumulated permanent deformation,
K_1 = ϵ_p at N = 1,
N = number of cycles at measured permanent deformation, and
m = slope of the log ϵ_p - log N relationship.

By substituting $\epsilon_p' = \epsilon(t) - \epsilon_{VER}$, where $\epsilon(t)$ is the total deformation and ϵ_{VER} is the viscoelastic recoverable deformation, then

$$\epsilon(t) - \epsilon_{VER} = K_1 N^{1-m} \tag{27a}$$

Then substitute $\epsilon_{VER} = \sigma_1/E'$ in Equation 27a and rearrange terms to get

$$\sigma = E'[\epsilon(t) - K_1 N^{1-m}] \tag{27b}$$

Finally, substitute Equation 27b into Equation 25 to get

$$\epsilon_{p_{acc}} = K_2(\sigma,t)[\epsilon(t) - K_1 N^{1-m}] \tag{28}$$

where

$$K_2(\sigma,t) = \begin{cases} (E'/E_{p_o}) + (E'/\eta_2)t + n_1^2\,[E'/H(W_p)] & \text{if } \sigma > \sigma_{yield},\ t > 0 \\ (E'/E_{p_o}) + (E'/\eta_2)t & \text{if } \sigma < \sigma_{yield},\ t < 0 \\ E'/E_{p_o} & \text{if } \sigma < \sigma_{yield},\ t = 0 \\ (E'/E_{p_o}) + n_1^2\,[E'/H(W_p)] & \text{if } \sigma > \sigma_{yield},\ t = 0 \end{cases}$$

E' = retarded elastic creep modulus = $1/\left((1/E_2) + (1/E_1)\{1 - \mathrm{EXP}[(-E_1/1)t]\}\right)$, and

N_D = design number of load repetitions.

Recalling the principle of exhaustion of ductility, then $\varepsilon(t)$ could be found from any monotonic stress-strain diagram such as those routinely used in asphalt mix testing. The important contribution here is that $K_2(\sigma,t)$ in Equation 28 reflects the effects of the different constitutive mechanisms to the accumulation of a rut depth that, in turn, rationalize decision alternatives. For example, if the contribution of densification is more dominant than that of the viscous and plastic deformations, then a decision on raising the compaction level of the asphalt mix pavement is rationalized. Similarly, if plastic deformation is dominant, then a decision to reduce contact stress or stiffen the mix with admixtures could be made. On the other hand, if viscous deformation is dominant, then consideration can be given to improving the asphalt cement (AC) viscosity by mixing grades or using additives. And if the ranges of K_1 and m can be established, then a design scheme for rutting could be implemented. In the next section an example is presented to show numerically how the procedure given in this section is used in calculating the laboratory-evaluated permanent deformation.

EXPERIMENTATION

Materials, Specimen Preparation, and Testing Program

This phase consisted of five laboratory-prepared recycled asphalt concrete mixes and their respective extracted field cores. Specific information on the mixes is given in Table 1.

The percentage of rejuvenator in the mix was selected on the basis of constructing viscosity design nomographs, which were used by targeting at a blend of 2000 poises absolute viscosity at 140°F to obtain the required percentage of rejuvenator (26). A total of 295 laboratory samples were prepared to conduct various tests, such as

1. Diametral modulus of resilience (MR) on Marshall-sized samples at 40°, 70°, and 100°F;
2. Indirect tensile strength (σ_{It}) using the same type samples and test temperatures as used for MR;
3. Unconfined compressive strength (q_u) on 4 x 4-in. cylinders at 70°F;
4. Incremental static compression rutting-creep test on 4 x 8-in. cylinders at 40°, 70°, and 100°F; modification is included (22) to account for determination of the friction element parameters in compression; and
5. Incremental static indirect tension rutting-creep test on cylinderical discs 4 in. in diameter by 2.5 in. in height at 70°F; modification is included (22) to account for determination of the friction element parameters in tension.

The test results from these series of tests are summarized in Tables 2 and 3.

MODEL VERIFICATIONS

Verification of Viscoelastic-Plastic Model

Elasto-Plastic Unit

Characterization of this model requires determining the yield condition parameters (α and K) and the hardening coefficient H. This is done as follows. First, the yield condition parameters are determined. The data in Table 1 summarize the results obtained on mixes 1 through 5 and give the MR, σ_{It}, and q_u values for the laboratory-fabricated samples and the two extracted field core assignments (1st assignment taken immediately after construction and 2nd assignment taken one year later). Tests were conducted at 40°, 70°, and 100°F for the MR and σ_{It}. The following example uses the Florida mix (mix 1).

Step 1: Direct Application of Classical Theory of Plasticity

Use Equation 17 to obtain

$$\pm\sigma_1 = 3K_o/[\alpha + \sqrt{3}\ \mathrm{sgn}(\sigma_1)] = \begin{cases} -802 \text{ psi compression} \\ +160 \text{ psi tension} \end{cases}$$

Then the following is obtained: $\alpha = 1.156$, $K_o = 154$ psi, and arctan α = 49.1°. Then substitute Equation 19 to get

$$n_1^2 = \begin{cases} 0.9802 \text{ in tension} \\ 0.039 \text{ in compression} \end{cases}$$

TABLE 1 Mix Information

Mix No.	Location	State	Mix Proportions		Rejuvenator
			Reclaimed %	New Agg. %	Type, % / %aged Asphalt
1	SR-91	Florida	65	35	AER, 38% / 62%
2	I-94	Michigan	85	15	AC-5, 81% / 19%
3	M-55(a)	Michigan	50	50	AC-20, 54% / 46%
4	M-55(b)	Michigan	50	50	AC-20, 45% Cyclogen, 10% / Aged Asphalt, 45%
5	M-55(c)	Michigan	50	50	Sulfur, 60% / 40%

TABLE 2 Test Results Summary (σ_{It}, MR, q_u, I)

		MIX No. 1			MIX No. 2			MIX No. 3			MIX No.4	MIX No.5
		LAB	FIELD 1st ass.	FIELD 2nd ass.	LAB	FIELD 1st ass.	FIELD 2nd ass.	LAB	FIELD 1st ass.	FIELD 2nd ass.	LAB	LAB
σ_{IT} psi	40°F	243.42	306.19	274.40	232.02	291.8		238.48	305.23	303.40	235.40	231.19
	70°F	160.71	62.58	58.83	109.98	57.25	55.95	113.97	61.93	56.50	104.65	229.75
	100°F	39.57	15.74	16.93	19.79	9.28	26.5	15.19	16.58	11.13	17.10	3.567
MR x 10^6 psi	40°F	1.352	2.61	2.27	1.304	2.97	2.82	1.146	3.74	3.33	0.418	3.567
	70°F	0.607	0.706	1.07	0.541	0.92	0.82	0.26	0.93	1.26	0.248	2.018
	100°F	0.203	0.303	0.193	0.061	0.123	0.104	0.033	0.145	0.168	0.037	1.256
Immersion Compress. psi	q_u	763	528	706	432	565	484	546		883	480	613
	q^*	802	585	719	539	564	700	470		657	438	1004
	I%	95	90	98	80	100	69	100		100	100	61

q_u = unconfined compressive strength after immersing in water

q^* = unconfined compressive strength

$I = q_u / q^*$ = index of retained strength

TABLE 3 Strain from Uniaxial Compression Creep Tests (x 10^{-3} in./in.)

Stress psi	t = 1.0 sec.			t = 3.0 sec.			t = 10.0 sec.			t = 30 sec.			t = 100 sec.			t = 1000 sec.			Aver. Value
	ϵ_t			ϵ_t			ϵ_t			ϵ_t			ϵ_t			ϵ_t			
	ϵ_c	ϵ_{Po}	ϵ_{PL}	ϵ_c	ϵ_{Po}	ϵ_{PL}	ϵ_c	ϵ_{Po}	ϵ_{PL}	ϵ_c	ϵ_{Po}	ϵ_{PL}	ϵ_c	ϵ_{Po}	ϵ_{PL}	ϵ_c	ϵ_{Po}	ϵ_{PL}	ϵ_{PL}
20	.563	1.14	0.0	.625	1.14	0.0	.813	1.14	0.0	.9	1.14	0.0	1.063	1.14	0.0	1.375	1.14	0.0	0.0
40	1.12	2.28	0.0	1.25	2.28	0.0	1.63	2.28	0.0	1.8	2.28	0.0	2.13	2.28	0.0	2.75	2.28	0.0	0.0
60	1.69	3.52	0.0	1.88	3.52	0.0	2.44	3.52	0.0	2.7	3.52	0.0	3.19	3.52	0.0	4.13	3.52	0.0	0.0
80	2.56	5.895	.31	2.81	5.895	.31	3.52	5.895	.27	3.89	5.895	.23	4.4	5.895	.15	5.6	5.895	.1	.22
120	4.68	6.0	1.31	5.01	6.0	1.26	6.08	6.0	1.2	6.35	6.0	.95	7.0	6.0	.82	9.0	6.0	.74	1.04
160	7.31	6.0	2.81	7.7	6.0	2.7	9.23	6.0	2.73	9.81	6.0	2.61	10.5	6.0	2.0	13.59	6.0	2.59	2.68

ϵ_{PL} = plastic strain = $\epsilon t - J\{t\} \times \sigma - \epsilon_{PO}$

$J\{t\} = \{\{64.25 + 0.00475t\} - \{9.73e^{-0.0185t} + 8.97 \times e^{-0.13658t} + 16e^{-0.4688t}\}\}$ microin./in/p.s.i.

Hence,

$$H = n_1^2 (d\sigma_1/d\epsilon_{PL}) \tag{29}$$

Step 2: Modification to Step 1

Step 1 assumes that yielding commences when $\sigma = \pm\sigma_1$ (maximum compressive or tensile strength of the material). Intuitively, however, yielding starts at some level of $\sigma < |\sigma_1|$. Consequently, a yield value of the material in both tension (σ_{ypt}) and compression (σ_{ypc}) should be obtained and substituted instead of $\pm\sigma_1$. These values for asphalt concrete are found by plotting the relationship between the steady-state creep rate ($\dot{\epsilon}_{ss}$) of the creep data under different stress levels versus the stress.

The rationale for using this method to find the yield point of asphalt mixes is based on the findings of many investigators regarding factors affecting creep. One of the simplest relationships between stress and steady-state strain rate, found to apply for certain metals and alloys, is of the form

$$\epsilon_{ss} = A\sigma^n \tag{30}$$

where $\dot{\varepsilon}_{ss}$ is the steady-state creep strain rate and A,n are the material constants that are stress dependent.

Values of n have been reported in the range of 1 to 10. Asphalt mixes at low stress and strain levels are considered linear viscoelastic, that is, n = 1 and $A\sigma$ = constant. However, at high stress levels it becomes nonlinearly stress dependent. For a viscoelastic-plastic system, the friction slider represents the element that possesses material nonlinearity. Consequently, a plot of $\dot{\varepsilon}_{ss}$ versus σ should reveal the stress at which nonlinearity occurs; that is, the friction slider element activated. This stress level is termed the yield point, σ_{yp}. Figure 3 shows the $\dot{\varepsilon}_{ss}$ - σ relationship; as expected, the coefficient of the in-series dashpot of the fitted Burger mechanical model does not change value up to a stress level of 60 psi. This substantiates the previous linear viscoelasticity hypothesis of asphalt mixes. The same plot is made for the indirect tension creep tests where this test was found to be sufficiently sensitive to the stress level, such that this finding could not be detected. Back extrapolation to $\dot{\varepsilon}_{ss}$ = 0 gave the following values:

σ_{ypt} = 3 psi, σ_{ypc} = 75 psi.

Using these values instead of $\pm\sigma_1$ gives α = 1.599, K_o = 3.33 psi, arctan α = 57.9°, and

$$\eta_1^2 = \begin{cases} 0.9117 \text{ in tension} \\ 0.00145 \text{ in compression} \end{cases}$$

Such results are not compatible with those obtained under Mohr-Coloumb failure criteria. Determining the hardening coefficient will be done after determining the viscoelastic model parameters.

Determination of Viscoelastic Unit Parameters from Rutting-Creep Tests

Compression and tension rutting-creep tests were conducted on 4 x 8-in. (diameter x height) cylinders and 4 x 2.5-in. (diameter x height) discs, respectively. Test results are given in Table 3 and plotted in Figures 4 and 5, showing $\varepsilon(t)$ versus t for different stress levels. A mechanical model for the 20-psi stress level is found by using the nonlinear SAS regression program. From these fittings, the relationship $\varepsilon(t)$ versus t is found to be dependent on stress level. For stress levels of 20, 40, and 60 psi, the in-series dashpot and spring constants are identical, but Kelvin element constants vary. The SAS program was used to fit the creep data by an equation of the form

$$\epsilon(t) = \sigma\{\beta_0 + \beta_1 * t + \beta_2 [1 - EXP(-\beta_3 t)]\} \quad (31)$$

which corresponds to a Burger model type response under creep loading conditions. The SAS program gave the following result:

$$\epsilon(t) = (\sigma/10^6)\{29.55 + 0.00475\, t + 1.73\, [1 - EXP(-1949.6t)]\} \quad (32)$$

from which the mechanical Burger model coefficients are

η_2 = 2.105 x 10^8 psi-sec, E_2 = 3.384 x 10^5 psi.
η_1 = 2.958 x 10^8 psi-sec, E_1 = 5.767 x 10^5 psi.

To determine the hardening coefficient H from fitting creep data by a Burger model, the creep compliance in uniaxial compression J(t) is calculated at the lowest stress level (20 psi) and by the linearity assumption; this creep compliance is independent of stress level. At higher stress levels, plastic deformation occurs and can be calculated from Equation 33, although a slightly different approach was adopted in the calculations in Table 3:

$$\epsilon_{PL} = \epsilon_p - \epsilon_{p_o} = \epsilon(t) - J(t) x \sigma - \epsilon_{p_o} \quad (33)$$

where

$\varepsilon(t)$ = total deformation,
ε_p = permanent deformation,
ε_{PL} = plastic deformation,
ε_{p_o} = permanent deformation due to densification,
σ = stress level, and
J(t) = creep compliance evaluated at the lowest stress level below the yield point.

The stress-average plastic strain relationship is given in Table 3 and is shown in Figure 6. The hardening coefficient is calculated and the results are

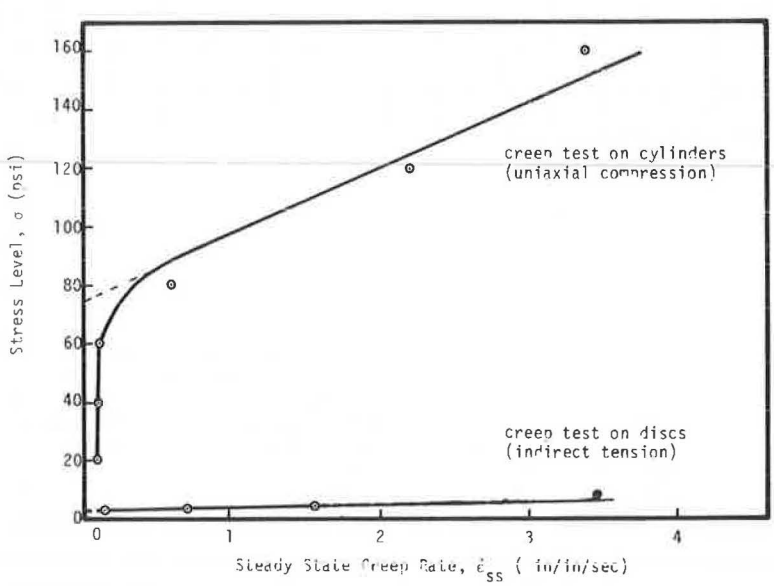

FIGURE 3 Steady-state deformation rate versus stress level curve.

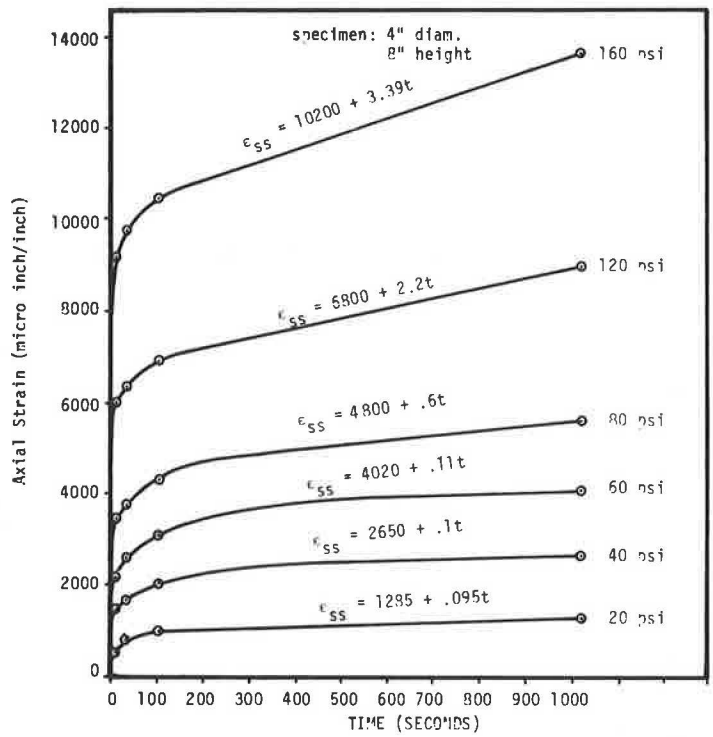

FIGURE 4 Compression rutting-creep.

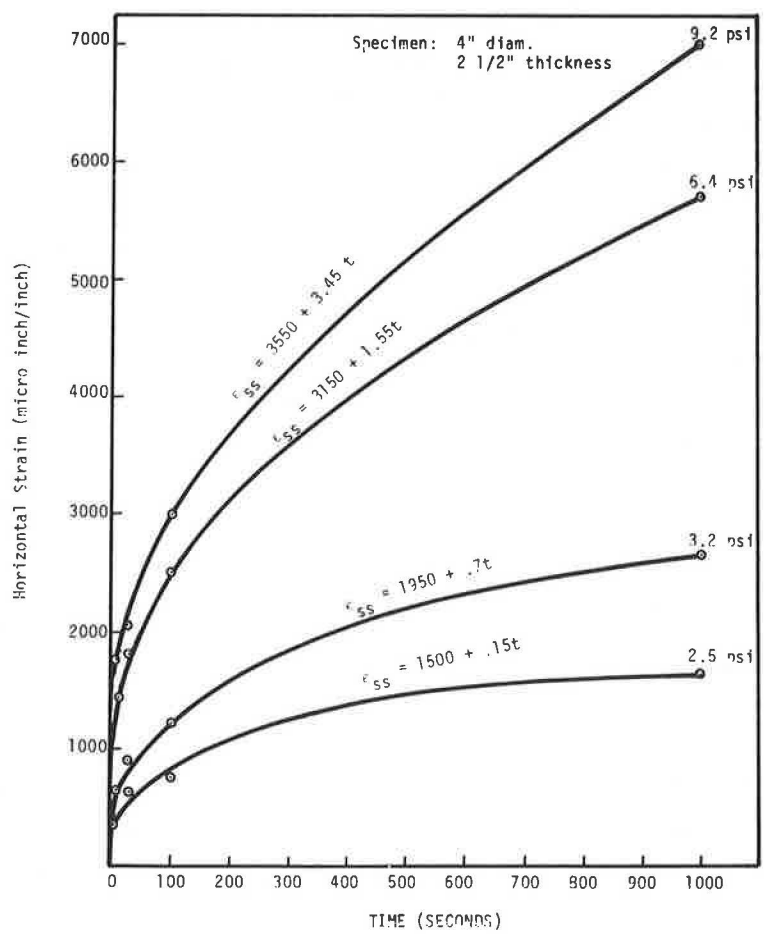

FIGURE 5 Indirect tension rutting-creep.

summarized in Table 4. The fitted equation is found by nonlinear SAS regression as

$$H(W_p) = 49.376 - 0.243W - 0.00043W^2 \quad (34)$$

This is plotted in Figure 7.

Summary of Example of Viscoelastic-Plastic Modeling

The model is summarized as follows:

$$\epsilon(t) = \sigma\{[1/(3.384 \times 10^5)] + [t/(2.105 \times 10^8)] + [1/(5.567 \times 10^5)](1 - e^{-1949.6t}) + <[n_1^2/H(W_p)]>\} \quad (35)$$

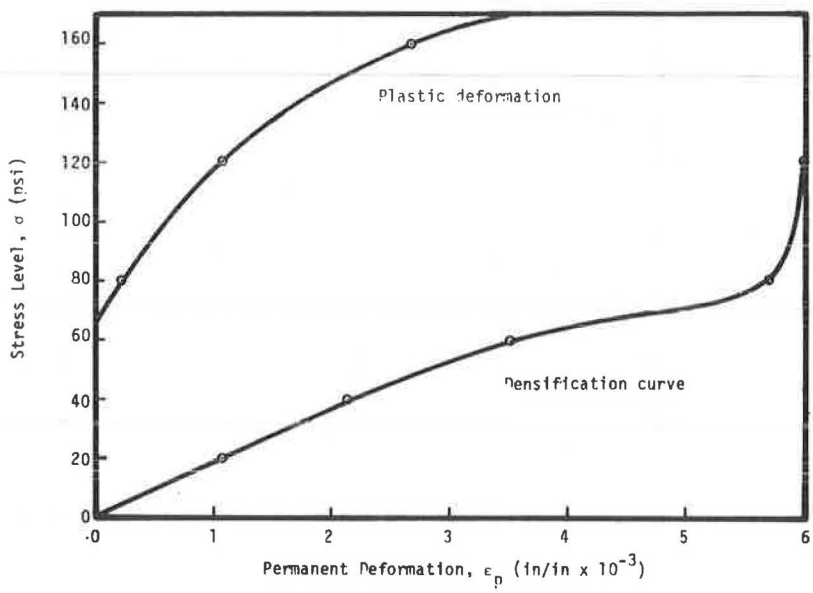

FIGURE 6 Permanent deformation versus stress level curve.

TABLE 4 Hardening Coefficient as a Function of Plastic Work Done

Stress level (psi)	20	40	60	80	120	160
$H \times 10^3$ (psi)	--	--	--	45.59	29.72	16.09
$W_p \times 10^{-3}$ (psi)	--	--	--	16.06	98.06	327.66

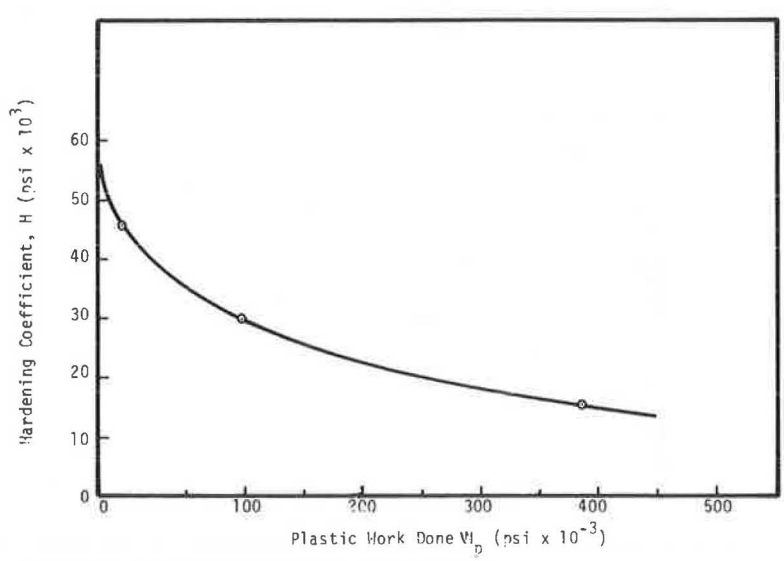

FIGURE 7 Hardening coefficient versus plastic work done curve.

where

$$H(W_p) = 49.38 - 0.243W_p + 0.00043W_p^2$$

$$n_1^2/H(W_p) = \begin{cases} 0 & \sigma_c < 75 \text{ and } \sigma_t < 3 \text{ psi} \\ 0.9117/H(W_p) & \sigma_t \geq 3 \text{ psi} \\ 0.00145/H(W_p) & \sigma_c \geq 75 \text{ psi} \end{cases}$$

RUTTING MODEL VERIFICATION

The rutting model requires determination of the permanent deformation versus number of cycles, in accordance with the dynamic series in VESYS II-M and the function $K_2(\sigma,t)$. The case of axial compression on 4 x 8-in. (diameter x height) samples is considered here. Test results are shown in Figure 8 on log-log scale, where the required relationship is found to be

$$\text{Log } \epsilon_p = 0.13 + 0.285 \log N \text{ in./in. x } 10^{-5} \quad (36)$$

from which the following is obtained:

$$\epsilon_p = 1.35N^{-0.715} \text{ in./in. x } 10^{-5} \quad (37)$$

Therefore, Equation 37 gives m = +0.715 and k_1 = 1.35 x 10^{-5} in./in.

The second step is to get $\epsilon(t)$ from monotonic testing or from creep test data (Table 3) at t = 100 sec: $\epsilon(t) = 10.445 \times 10^{-3}$ in./in.

The third step is to find the function $K_2(\sigma,t)$. This was done in the viscoelastic-plastic model with a yield surface model. The function is found to be

$$E' = 3.0656 \times 10^5 \text{ psi}$$

$$K_2(\sigma,t) = \{(1/E_{p_o}) + [1/(2.105 \times 10^8)]\, t + [0.00145/H(W_p)]\} \times 3.0656 \times 10^5$$

For σ = 80 psi representing the contact pressure of the design vehicle, $E_{p_o} = 5.7 \times 10^5$ psi (using Figure 6) and $H(W_p) = 45 \times 10^3$ psi (using Table 4). Therefore, $k_2(\sigma,t)$ = (0.53 + 0.145 + 0.01) = 0.693. This indicates that 77.6 percent of the total permanent deformation is due to densification, 1.5 percent due to plastic deformation, and 20.9 percent due to viscous deformation. Then substitute Equation 28 to get

$$\epsilon_{P_{acc}} = 0.693\,[10.445 \times 10^{-3} - (1.35/10^5)N^{1-0.715}] \text{ in./in.}$$

For N = 840,000 cycles, $\epsilon_{P_{acc}}$ = 0.678 percent, and accordingly, a 10-in.-thick pavement, it is expected to accumulate 0.0678 in. permanent deformation due to direct compression on the surface after 840,000 load repetitions. Such a result is compatible with those obtained by using the VESYS III structural subsystem program given in Table 5. The laboratory densification phase includes sources of error factors such as seating and conditioning that do not occur or match those in the field, however.

CONCLUSIONS

1. A combo viscoelastic-plastic model has been developed to characterize asphalt mixes. The model parameters are easily found by simple adjustments, modifications, or extensions of existing routine testing schemes. Among the findings when developing this model were the following: (a) a true yield surface could be found and used instead of that of the Mohr-Coloumb failure surface, and (b) as a consequence of (a) and specific to the tested mix, yielding occurs at about 75 psi in compression and 3 psi in tension at 70°F. On this basis it is recommended that stress levels of less than 3 psi be used to find the MR. Further, plastic deformation should be accounted for in characterization because actual stress levels on pavement surfaces exceed 75 psi.

2. A Drucker-Prager true yield surface was identified and its parameters found experimentally.

3. A rutting model based on the viscoelastic-plastic characterization has been developed. The example illustrated the application of this model to predict rutting of laboratory-prepared asphalt mixes. Among the conclusions is that permanent deformation due to densification is better included in rut depth calculations based on laboratory and field measurement simulations. Further, densification permanent deformation could be represented by an elastic relaxing spring.

4. Test methods that use the incremental static series do not differentiate between densification and the rest of nonrecoverable deformation. However, a procedure was established in this work to accomplish that. Differentiating quantitatively between densification, viscous, and plastic deformation is

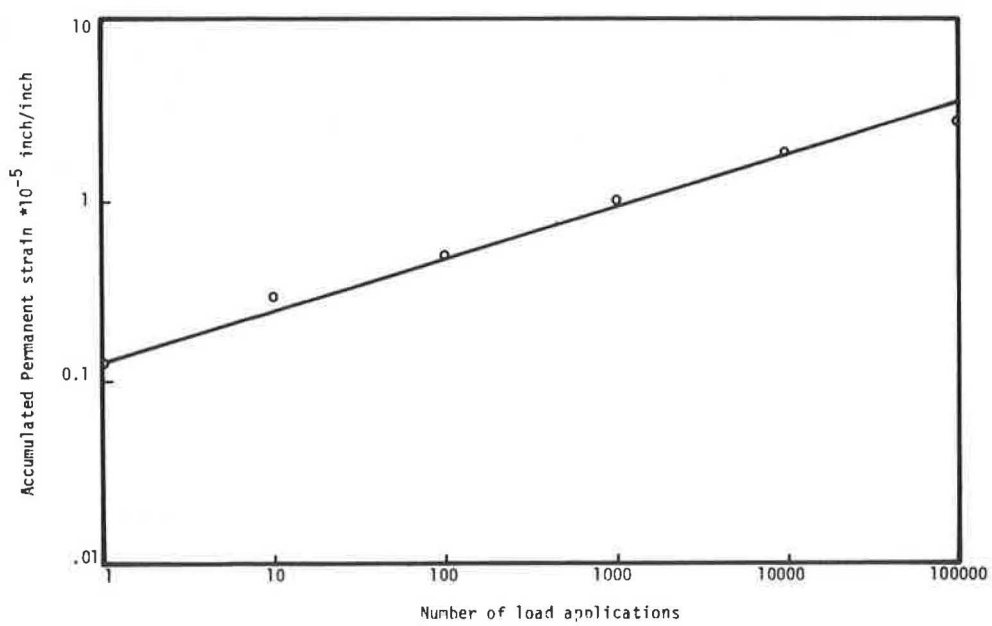

FIGURE 8 Rutting dynamic test series.

TABLE 5 Rut Depth in Inches, Using VESYS III

Traffic axle loads in 20 years	1.4 million			3.5 million	7 million		
Thickness (in) / No. of years	6	8	10	6	6	8	10
1/2	.036	.032	.029	.044	.051	.046	.042
2	.057	.056	.054	.071	.083	.08	.078
12	.086	.083	.082	.106	.124	.12	.118
20	.097	.094	.092	.119	.14	.135	.132

expected to rationalize decision alternatives for field problems, and hence, to implement asphaltic mix design.

REFERENCES

1. C.F. Rogers, H.D. Cashell, and P.E. Irick. Nationwide Survey of Pavement Terminal Serviceability. In Highway Research Record 42, HRB, National Research Council, Washington, D.C., 1963, pp. 26-40.
2. J. Morris et al. Permanent Deformation in Asphalt Pavements Can Be Predicted. Proc., Association of Asphalt Paving Technologists, Vol. 45, 1974.
3. K. Majidzadeh et al. Development and Field Verification of a Mechanistic Structural Design System in Ohio. Proc., 4th International Conference on Structural Design of Asphalt Pavements, Vol. 1, 1977.
4. K. Majidzadeh et al. Application of Fracture Mechanics for Improved Design of Bituminous Concrete. Report RF3736. Ohio State University, Columbus, 1976.
5. M. Karakouzian. A Simplified Method for Material Testing and Design of Pavement Systems. Ph.D. dissertation. Ohio State University, Columbus, 1978.
6. C.I. Monismith. Viscoelastic Behavior of Asphalt Concrete Pavements. Proc., International Conference on Structural Design of Asphalt Pavements, 1963.
7. H.S. Papazian. The Response of Linear Viscoelastic Materials in the Frequency Domain with Emphasis on Asphalt Cement. Proc., International Conference on Structural Design of Asphalt Pavements, 1965.
8. K.E. Secor and C.L. Monismith. Viscoelastic Response of Asphalt Paving Slabs Under Creep Loading. In Highway Research Record 67, HRB, National Research Council, Washington, D.C., 1965, pp. 84-97.
9. J.P. Elliot and F. Moavenzadeh. Moving Load on Viscoelastic Layered Systems: Phase II. Report 69-64. Department of Civil Engineering, Massachusetts Institute of Technology, Cambridge, 1969.
10. W.J. Kenis. Predictive Design Procedures, VESYS User's Manual: An Interim Design Method for Flexible Pavements Using the VESYS Structural Subsystem, Final Report. Report FHWA-RD-77-154. FHWA, U.S. Department of Transportation, 1978.
11. W.J. Kenis. Predictive Design Procedures: VESYS User's Manual. Report FHWA-RD-77-154. FHWA, U.S. Department of Transportation, Aug. 1980.
12. S.R. Bonder and Y. Partom. Constitutive Equations for Elastic-Viscoplastic Strain Hardening Materials. ASME, Journal of Applied Mechanics, Vol. 42, 1975, p. 385.
13. K.C. Valanis. A Theory of Viscoplasticity Without a Yield Surface--Part I: General Theory, Part II: Applications to Mechanical Behavior of Metals. Archiwum Mechaniki Stosowanej, Vol. 24, 1971.
14. D.R.J. Owen and E. Hinton. Finite Element in Plasticity: Theory and Practice. Pineridge Press Ltd., Swansea, England, 1980.
15. O.C. Zienkiewicz and I.C. Cormeau. Viscoplasticity, Plasticity, and Creep in Elastic Solids--A Unified Numerical Solution Approach. International Journal of Numerical Methods in Engineering, Vol. 8, 1974, pp. 821-824.
16. O.C. Zienkiewicz, V. Norris, and D.J. Naylor. Plasticity and Viscoplasticity in Soil Mechanics with Special Reference to Cyclic Loading Problems. Proc., International Conference on Finite Elements in Nonlinear Solid and Structural Mechanics, Aug. 1977, pp. 455-485.
17. R.D. Barksdale. Laboratory Evaluation of Rutting in Base Course Materials. Proc., 3rd International Conference on Structural Design of Asphalt Pavements, 1972.
18. M.R. El-Mitiny. Material Characterization for Studying Flexible Pavement Behavior in Fatigue and Permanent Deformation. Ph.D. dissertation. Ohio State University, Columbus, 1980.
19. K. Majidzadeh, F. Bayomy, and S. Khedr. Rutting Evaluation of Subgrade Soils in Ohio. In Transportation Research Record 671, TRB, National Research Council, Washington, D.C., 1978, pp. 75-84.
20. A. Phillips and G.J. Weng. An Analytical Study of Experimentally Verified Hardening Law. ASME, Journal of Applied Mechanics, Vol. 42, 1975.
21. W. Prager. An Introduction to Plasticity. Addison-Wesley, Reading, Mass., 1959.
22. A. Abdulshafi. Viscoelastic/Plastic Characterization, Rutting, and Fatigue of Flexible Pavements. Ph.D. dissertation. Ohio State University, Columbus, 1983.
23. M. Katona. Viscoelastic-Plastic Constitutive Model with a Finite Element Solution Methodology. Report TR-866. Civil Engineering Labora-

tory, Naval Construction Battalion Center, Port Hueneme, Calif., 1978.
24. O.C. Zienkiewicz. The Finite Element Method. McGraw-Hill, New York, 1972.
25. E.J. Yoder and M.W. Witczak. Principles of Pavement Design. Wiley, New York, 1975.
26. A.A. Abdulshafi. Rheological Behavior of Rejuvenated Aged Asphalt. M.S. thesis. Ohio State University, Columbus, 1981.

Publication of this paper sponsored by Committee on Characteristics of Bituminous Paving Mixtures to Meet Structural Requirements.

Evaluation of Tests for Characterizing the Stiffening Potential of Baghouse Dust in Asphalt Mixes

DAVID A. ANDERSON and STEVEN M. CHRISMER

ABSTRACT

Since the enactment of the 1970 Clean Air Act many asphalt plants have been forced to install baghouse dust collectors. Often this dust is added to asphalt concrete mixtures. The dust can stiffen mixes, thereby making them hard to compact, or it can act as an extender, thus causing bleeding and tenderness. There are no accepted specification tests for controlling the stiffening or the extending effects of baghouse dust. A variety of simple test procedures were evaluated for possible use for specification or quality control purposes to control stiffening. The customary physical properties of the dust, such as pH, shape, and gradation, do not predict stiffening. Two types of test procedures--fractional voids and consistency--were correlated with stiffening as measured by the increase in viscosity or softening point caused by the addition of dust to asphalt cement. Fractional voids in dust-asphalt mixtures were calculated from the bulk volume of dust compacted with impact and vibratory compaction and by consolidation in fluid media. Consistency tests included the kerosene, balling and crumbling, and bitumin number tests. The best correlation with stiffening ratio was obtained from the fractional voids as determined from the dry impact compaction. This test procedure is acceptable for process control and acceptance procedures; the other test procedures are not acceptable. The best means of determining the stiffening effect is to determine the stiffening directly with capillary viscometry. However, before either the fractional void test or the direct measure of stiffening is included as a specification criteria for stiffening, they must be determined through correlation with field performance.

Since the enactment of the 1970 Clean Air Act the operators of many asphalt concrete plants have found it necessary to install secondary dust-collection systems. These systems collect the fine dust that would otherwise be released from the exhaust gas to the atmosphere. Filter fabric dust collectors are the most commonly used secondary collection systems. They are usually referred to as baghouses, and the collected dust is called baghouse dust. Baghouse dust may be extremely fine (1 μm to 30 μm) or it may contain a wide range of particle sizes (1 μm to 300 μm), according to the configuration of the plant (1). Finer dust is produced when a cyclone or other type of primary collector is used in series with a baghouse. The cyclone collector effectively removes dust larger than 30 μm, thereby stripping the coarser fraction from the dust collected in the baghouse. Therefore, baghouse dust from different plants can vary widely in gradation.

Baghouse dust often presents a disposal problem, and in many plants it is common to add baghouse dust to the asphalt concrete. Some paving technologists are reluctant to do this because they believe that the dust can adversely affect the quality of the asphalt concrete. For example, baghouse dust can act as an asphalt extender, thus reducing the design asphalt content. If the addition of baghouse dust is not accounted for in the mix design, bleeding and tenderness can result (2,3).

Other problems that have been attributed to the improper use of baghouse dust include poor compaction and raveling resulting from excessive stiffening of the asphalt concrete (4-6). Concern about the stiffening effect of baghouse dust has led many highway agencies to restrict its use (7). Other agencies have adopted or are considering test procedures that are intended to control the use of baghouse dust (8). These test procedures are designed primarily to control mixture stiffening caused by baghouse dust.

The purpose of this paper is to report on a laboratory evaluation of several test procedures that measure the stiffening of asphalt cement that results from the addition of a fine mineral dust. The